ELSEVIER

Journal of Alloys and Compounds 434–435 (2007) 152–155

Journal of ALLOYS AND COMPOUNDS

www.elsevier.com/locate/jallcom

Estimation of the glass forming ability of the Ni–Zr and the Cu–Zr alloys

Taichi Abe *, Masato Shimono, Machiko Ode, Hidehiro Onodera

Computational Materials Science Center, National Institute for Materials Science, 1-2-1 Sengen, Tsukuba, Ibaraki 305-0047, Japan

Available online 29 September 2006

Abstract

Thermodynamic assessments of the Ni–Zr and the Cu–Zr binary systems were carried out using thermodynamic properties obtained in a wide range of temperatures. The associated solution model was applied to describe the short range ordering in the liquid. The critical cooling rates for the glass formation were estimated from the optimized parameter set, and compared with experimental data. In both the Cu–Zr and the Ni–Zr systems, the minimum critical cooling rate was found in alloys with compositions around 35 at.% Zr. Smaller critical cooling rates in the Cu–Zr system than those in the Ni–Zr alloys suggest that Cu–Zr alloys have higher GFA than Ni–Zr alloys.

Keywords: Metallic glasses; Crystallization; Short range ordering; Critical cooling rate

1. Introduction

The bulk metallic glasses have been found in various alloy systems [1]. It has been investigated intensively in recent years, in order to improve glass forming ability (GFA) of those glassy alloys and to explore alloys with higher GFA. Variety of bulk glassy alloy systems with high GFA has been found since the late 1980s. The GFA has usually been discussed by the following indicators: undercooled liquid range, reduced glass transition temperature, the critical cooling rate, and the driving force for the crystallization from the undercooled liquid. Those indicators have been evaluated from experiments and from thermodynamic calculations [2].

The CALPHAD method has been widely employed in research on the phase diagrams of various alloy systems [3,4]. Accumulation of thermodynamic data and compilation of thermodynamic databases have enabled various kinds of thermodynamic analyses. Using those thermodynamic databases, several attempts have been made to estimate the GFA such as the driving force for crystallization from the undercooled liquid, and the critical cooling rate for the amorphous formation [5–7]. Recently, the authors have shown in the Cu–Zr binary systems [8] that those thermodynamic properties at low temperatures, which are missing in previous assessments of those binary systems [9–11], are indispensable for accurate estimation of the driving forces and the critical cooling rates.

In the present study, the liquid phase in the Ni–Zr and the Cu–Zr binary systems has been assessed using thermodynamic properties obtained in a wide range of temperatures by means of the CALPHAD method. Then, the driving force for the crystallization from the undercooled liquid, and the critical cooling rates for the glass formation were estimated, and compared with the experimental data.

2. Thermodynamic models

In the present study, the associated solution model was adopted for describing the effect of short range ordering in the liquid, and an associate Cu_2Zr_1 in the Cu–Zr binary system, and an associate Ni_2Zr_1 in the Ni–Zr binary system were assumed.

In a liquid X–Zr (X = Cu or Ni) binary alloy, it assumed that $n_{X_2Zr_1}$ moles of the associate X_2Zr_1, is in equilibrium with the n_X and n_{Zr} moles of free X and Zr atoms, respectively. The excess Gibbs free energy of mixing, G_m^{ex}, is given by

$$G_m^{ex} = n_{X_2Zr_1} G^0_{X_2Zr_1} + \frac{n_X n_{Zr}}{n} G^{reg}_{X,Zr} + \frac{n_X n_{X_2Zr_1}}{n} G^{reg}_{X,X_2Zr_1} + \frac{n_{X_2Zr_1} n_{Zr}}{n} G^{reg}_{X_2Zr_1,Zr} + RT\left(n_X \ln\frac{n_X}{n} + n_{Zr} \ln\frac{n_{Zr}}{n} + n_{X_2Zr_1} \ln\frac{n_{X_2Zr_1}}{n}\right) + \Delta G_m^{L\text{-}Am} \quad (1)$$

where $G^0_{X_2Zr_1}$, T, R and n are Gibbs free energy change due to the formation of the associate, temperature, the gas constant and the sum of moles of atoms and associates given by

* Corresponding author. Tel.: +81 29 859 2628; fax: +81 29 859 2601.
E-mail address: abe.taichi@nims.go.jp (T. Abe).

0925-8388/$ – see front matter © 2006 Elsevier B.V. All rights reserved.
doi:10.1016/j.jallcom.2006.08.172

$n = n_X + n_{Zr} + n_{X_2Zr_1}$, respectively. G^{reg}_{X,X_2Zr_1}, $G^{reg}_{X_2Zr_1,Zr}$, and $G^{reg}_{X,Zr}$ are the Gibbs free energies due to the interactions among components given by the Redrich–Kister polynomials as

$$G^{reg}_{i,j} = \sum_{v=0}^{k} L^{v}_{i,j}\left(\frac{n_i}{n} - \frac{n_j}{n}\right)^v \quad (2)$$

where $L^v_{i,j}$ are an interaction parameters between components i and j, and were fitted to experimental data.

For the glass transition, the thermodynamic model proposed by Shao [12] has an advantage that the glass transition temperature can be fitted directly to experimental data and thus was adopted in the present assessment. In his model, the glass transition is treated as a second order transition with Hillert–Jarl functions [13]. The Gibbs free energy change due to the glass transition is presented in the following equations:

$$\Delta G^{L\text{-}Am}_m = -RT_g \ln(1+\alpha) f(\tau), \quad (3)$$

where τ, α, and $f(\tau)$ are temperature normalized by the glass transition temperature T_g, a factor due to the amorphization, and Hillert–Jarl function, respectively. α and T_g are composition dependent and, for the X–Zr binary liquid, are given by following equations:

$$T_g = n_X T^X_g + n_{Zr} T^{Zr}_g + n_{X_2Zr_1} T^{X_2Zr_1}_g + n_X n_{Zr} \Omega^{X,Zr}_0 + n_X n_{X_2Zr_1} \Omega^{X,X_2Zr_1}_0 + n_{X_2Zr_1} n_{Zr} \Omega^{X_2Zr_1,Zr}_0 \quad (4a)$$

$$\alpha = n_X \alpha_X + n_{Zr} \alpha_{Zr} + n_{X_2Zr_1} \alpha_{X_2Zr_1} + n_X n_{Zr} \Lambda^{X,Zr}_0 + n_X n_{X_2Zr_1} \Lambda^{X,X_2Zr_1}_0 + n_{X_2Zr_1} n_{Zr} \Lambda^{X_2Zr_1,Zr}_0 \quad (4b)$$

where α_i, T^i_g, $\Lambda^{i,j}_0$, and $\Omega^{i,j}_0$, are constants.

In the Ni–Zr and the Cu–Zr systems, the Gibbs free energies of the intermetallic compounds have been well determined by Zaitsev et al. [14,15]. Thus, in the present study, the thermodynamic assessment of the liquid phase was carried out keeping these Gibbs free energies of the intermetallic phases fixed in the assessment. The parameters in Eqs. (1)–(4) were fitted to experimental data such as enthalpy of mixing in the liquid, formation enthalpy of amorphous, heat capacity, and latent heat for crystallization, using Parrot module in the Thermo-Calc software package.

Table 1
Optimized thermodynamic parameters for the liquid in the Cu–Zr and the Ni–Zr systems (G and L in J/mol, and T and Ω in K)

$G^0_{Ni_2Zr_1} = -72000 + 20T$	$G^0_{Cu_2Zr_1} = -38110 + 16.7T$
$L^0_{Ni,Zr} = -170700 + 13.4T$	$L^0_{Cu,Zr} = -61890 + 16.2T$
$L^1_{Ni,Zr} = -90000 + 40T$	$L^0_{Cu,Cu_2Zr_1} = -96100 + 72.4T$
$L^0_{Ni,Ni_2Zr_1} = -295000 + 180T$	$L^0_{Cu_2Zr_1,Zr} = -177800 + 134.4T$
$L^0_{Ni_2Zr_1,Zr} = -278000 + 73T$	
$T^{Ni}_g = 1035$	$\alpha_{Ni} = 2.416^*$
$T^{Zr}_g = 444$	$\alpha_{Zr} = 3.306^*$
$T^{Cu}_g = 795$	$\alpha_{Cu} = 2.183^*$
$T^{Cu_2Zr_1}_g = 620$	$\alpha_{Cu_2Zr_1} = 16.6$
$T^{Ni_2Zr_1}_g = 855$	$\alpha_{Ni_2Zr_1} = 32$
$\Omega^{Cu,Zr}_0 = 0$	$\Lambda^{Ni,Zr}_0 = 15$
$\Omega^{Ni,Zr}_0 = 0$	$\Lambda^{Cu,Zr}_0 = 22.4$
$\Omega^{Cu,Cu_2Zr}_0 = 62.8$	$\Lambda^{Ni,Ni_2Zr_1}_0 = -58$
$\Omega^{Cu_2Zr_1,Zr}_0 = 380$	$\Lambda^{Ni_2Zr_1,Zr}_0 = -58$
$\Omega^{Ni,Ni_2Zr_1}_0 = -290$	$\Lambda^{Cu,Cu_2Zr_1}_0 = -57.58$
$\Omega^{Ni_2Zr_1,Zr}_0 = 510$	$\Omega^{Cu_2Zr_1,Zr}_0 = -20.23$

Parameters with an asterisk are taken from Shao [12].

3. Results and discussions

3.1. The driving force for the crystallization

A phase having the largest driving force is expected to form as the primary crystalline phase at the crystallization temperature. Therefore, the driving force seems to be a candidate of the indicator to show the GFA. Using the obtained parameter set for the liquid listed in Table 1, the driving forces for the crystallization in the Cu–Zr, and in the Ni–Zr systems at 800 K, were calculated, and shown in Fig. 1(a and b), respectively.

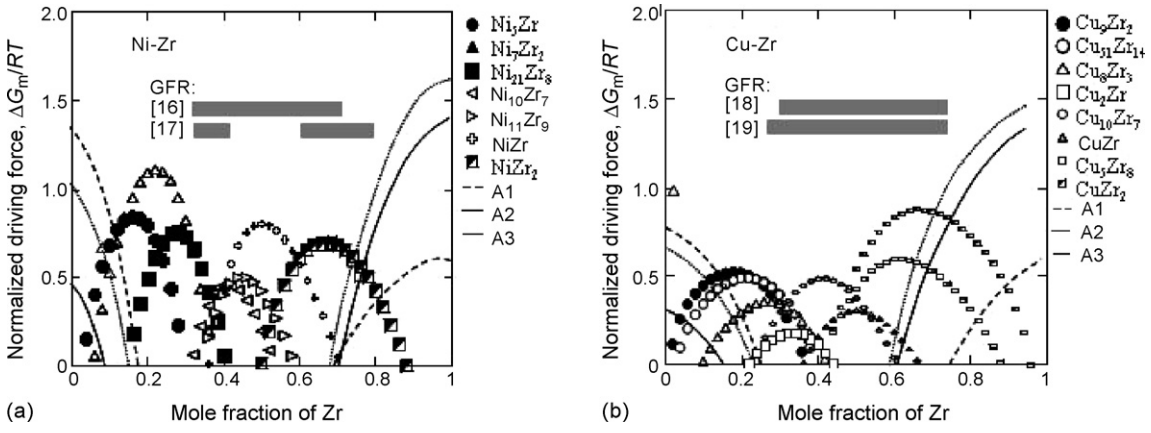

Fig. 1. Driving force for crystallization of the crystalline phases from the undercooled liquid at 800 K along with the experimental GFR (a) in the Ni–Zr system, and (b) in the Cu–Zr system.

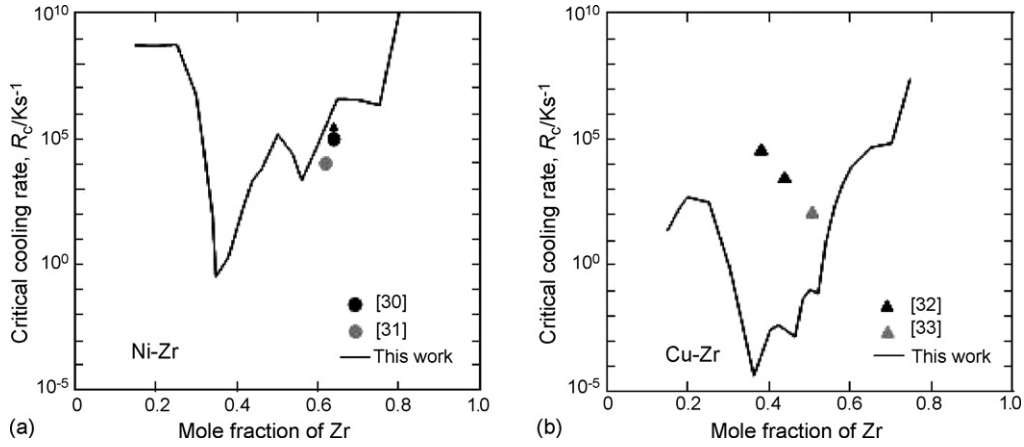

Fig. 2. The calculated critical cooling rates along with the experimental data (a) in the Ni–Zr system and (b) in the Cu–Zr system.

Experimental glass forming ranges (GFR) [16–19] in those binary systems are shown in the figures as well. In the Ni–Zr system, the GFR by Dong et al. [17] reported that the amorphous does not form at around the 50 at.% Zr, where the relatively low GFA is expected from the high driving force for the formation of the NiZr compound. The experimental GFR in the both Ni–Zr and Cu–Zr systems agree well with the composition ranges of the smaller driving forces for the crystallization as shown in Fig. 1(a and b).

It has been experimentally observed that the Cu–Zr alloys [20] show the distinct glass transition on the DSC heating curve, while it is difficult to observe it in the Ni–Zr alloys. The driving forces in the Ni–Zr alloys are higher than those in the Cu–Zr alloys almost all compositions, suggesting that the Cu–Zr alloys have higher GFA than the Ni–Zr alloys.

3.2. The critical cooling rate for the glass formation

Several attempts have been made to estimate the Time–Temperature-Transformation (T.T.T.) curve for the crystallization [5,21–24]. According to Saunders and Miodownik [5], the time, t, necessary to form the volume fraction of X_v is given by the Johnson–Mehl–Avrami equation as

$$t = \frac{44.3\eta}{kT}\left\{\frac{r_0^9 X_v}{f^3 N_v}\frac{\exp(G^*/kT)}{[1-\exp(-G_m/RT)]^3}\right\}^{1/4}, \quad (5)$$

where r_0, f, N_v, η, G^*, and G_m are an atomic radius, a structural constant, the number of atoms per unit volume, the viscosity, the free energy barrier for the nucleation, and the driving force of the crystallization from the liquid, respectively. The thermodynamic factors, G^* and G_m, were estimated from the optimized parameter set. The free energy barrier for the nucleation is given by the term σ_m is the solid–liquid interfacial energy, and has been related to the molar heat of fusion,

$$G^* = \frac{16\pi}{3N_v}\frac{\sigma_m^3}{G_m^2}, \quad (6)$$

H_m^f, such that $\sigma_m = \alpha_m H_m^f$, where α_m was empirically evaluated to be approximately 0.41 [5]. For the viscosity of the undercooled liquid, the Vogel–Fulcher equation was applied, coefficients in the equation were fitted to reproduce experimental data [25–27].

Fig. 2(a and b) show the critical cooling rates for the Ni–Zr and the Cu–Zr alloys as a function of Zr. The minimum critical cooling rate found at 35 at.% Zr in the Cu–Zr system, and at 35 at.% Zr in the Ni–Zr systems suggests that those alloys have higher GFA than alloys with other compositions.

According to the results of the molecular dynamic (MD) simulations [28,29], for the case of an A–B binary liquid where an A atom is 20% smaller in radius than that of a B atom, the maximum packing density in the undercooled liquid is obtained at around 35 at.% B. They have found that the higher packing density gives the higher coordination number and the lower atomic mobility, and thus results in the lower internal energy and the higher kinematical stability of the system. Here in the present case, the driving force for the nucleation decreases with decreasing the free energy of the undercooled liquid because the stoichiometric compound forms in the crystallization. The atomic radius of Zr is 20% and 18% larger than tat of Cu and Ni, respectively. Thus, their results explain very well the present calculations that the highest glass forming abilities are expected at around 35 at.% Zr for both systems.

Since the critical cooling rates in the Ni–Zr system are much faster than those in the Cu–Zr systems, the GFA of Cu–Zr alloys is higher than that of Ni–Zr alloys as observed in the experiments [20]. The reason for the lower GFA of Ni–Zr alloys is explained as follows. The parameters, viscosity, the interfacial energy, and the driving force in Eq. (5) depend on alloy systems. The estimated solid–liquid interfacial energies the Ni–Zr system are larger than those in the Cu–Zr system by a factor of 2, and this leads to the slower critical cooling rates in the Ni–Zr system. However, the critical cooling rates in the Ni–Zr system are much faster than those in the Cu–Zr system. For the viscosity, according to the experimental data [25–27], the difference in those binary systems is small. Thus, it can be concluded that the higher driving forces in the Ni–Zr alloys than those in the Cu–Zr alloys, as shown in Fig. 1(a and b), are responsible for the lower GFA of Ni–Zr alloys.

In the present case, although the thermodynamic properties at low temperatures were properly taken into account, the critical cooling rates estimated in the present assessment are slower than those experimental data [30–33]. This suggests that the crystallization occurs much faster than that expected from the homogeneous nucleation theory. One of possible explanations for this large discrepancy would be that the heterogeneous nucleation from the undercooled liquid is dominant where defects, inclusions, and short range ordered structures such as an icosahedral cluster can be potential heterogeneous nucleation sites. Thus, for more quantitative discussions, the investigations on atomic configurations in the undercooled liquids including the short range ordering and their relations to the nucleation processes are needed.

4. Conclusions

The thermodynamic assessments of the liquid in the Ni–Zr and the Cu–Zr binary systems were carried out. The driving force and the critical cooling rates for the amorphous formation were estimated from the assessed Gibbs energy functions of the liquids.

In both the Cu–Zr and the Ni–Zr systems, the minimum critical cooling rate was found in alloys with composition of 35 at.% Zr. The critical cooling rates in the Cu–Zr alloys are smaller than those in the Ni–Zr alloys, suggesting that Cu–Zr alloys have higher GFA than Ni–Zr alloys. Comparing to the critical cooling rates in those two binary systems, it was shown that the GFA of Cu–Zr alloys are higher than that of Ni–Zr alloys.

Acknowledgments

The present research is partly supported by Grant-in-Aid for Scientific Research (No. 428-15074220) from Japan Society for the Promotion of Science. The support from Core Research for Evolutional Science and Technology (CREST), Japan Science and Technology Agency, is acknowledged.

References

[1] A. Inoue, Acta Mater. 48 (2000) 279.
[2] A. Takeuchi, A. Inoue, Mater. Sci. Eng. A 375–377 (2004) 449.
[3] B. Sundman, B. Jansson, J.-O. Andersson, CALPHAD 9 (1985) 153.
[4] N. Saunders, A.P. Miodownik, CALPHAD—Calculation of Phase Diagrams, a Comprehensive Guide, Elsevier Science, Oxford, 1998.
[5] N. Saunders, A.P. Miodownik, Mater. Sci. Technol. 4 (1988) 768.
[6] R. Bormann, F. Gärtner, K. Zöltzer, J. Less Common Met. 145 (1988) 19.
[7] W. Sha, J. Alloys Compd. 322 (2001) L17.
[8] T. Abe, H. Onodera, M. Shimono, M. Ode, Mater. Trans. 46 (2005) 2838.
[9] G. Ghosh, J. Mater. Res. 9 (1994) 598.
[10] K.J. Zeng, M. Hämäläinen, H.L. Lukas, J. Phase Equilib. 15 (1994) 577.
[11] B.C. Anusionwu, G.A. Adebayo, J. Alloys Compd. 329 (2001) 162.
[12] G. Shao, J. Appl. Phys. 88 (2000) 4443.
[13] M. Hillert, M. Jarl, CALPHAD 2 (1978) 227.
[14] A.I. Zaitsev, N.E. Zaitseva, E.K. Shakhpazov, A.A. Kodentsov, Phys. Chem. Chem. Phys. 4 (2002) 6047.
[15] A.I. Zaitsev, N.E. Zaitseva, High Temp. 41 (2003) 42.
[16] J. Eckert, L. Schults, E. Hellstern, J. Appl. Phys. 64 (1988) 3224.
[17] Y.D. Dong, G. Gregan, M.G. Scott, J. Non-Cryst. Solids 43 (1891) 403.
[18] Z. Altounian, T. Guo-hua, J.O. Strom-Olsen, J. Appl. Phys. 53 (1982) 4755.
[19] C. Bergman, L. Komarek, CALPHAD 9 (1985) 1.
[20] J. Saida, M. Kasai, E. Matsubara, A. Inoue, Ann. Chim. Sci. Mat. 27 (2002) 77.
[21] H.A. Davies, Phys. Chem. Glasses 17 (1976) 159.
[22] D.R. Uhlmann, J. Non-Cryst. Solids 7 (1972) 337.
[23] H.G. Jiang, J. Baram, Mater. Sci. Eng. A A208 (1996) 232.
[24] T. Tokunaga, H. Ohtani, M. Hasebe, CALPHAD 28 (2004) 354.
[25] K. Ohsaka, S.K. Chung, W.K. Rhim, Acta Mater. 46 (1998) 4535.
[26] W.N. Myung, H.G. Kim, T. Masumoto, Mater. Sci. Eng. A A179–A180 (1994) 252.
[27] R. Novakovic, M.L. Muolo, A. Passerone, Surf. Sci. 549 (2004) 281.
[28] M. Shimono, H. Onodera, Scr. Mater. 44 (2001) 1595.
[29] M. Shimono, H. Onodera, Mater. Trans. 45 (2004) 1163.
[30] H.-J. Fecht, W.L. Johnson, Mater. Sci. Eng. A 375–377 (2004) 2.
[31] R. Busch, J. Miner. Met. Mater. Soc. 52 (2000) 39.
[32] F. Gillessen, D.M. Herlach, Mater. Sci. Eng. 97 (1988) 147.
[33] P. Yu, H.Y. Bai, M.B. Tang, W.L. Wang, J. Non-Cryst. Solids 351 (2005) 1328.